

Superconductivity beyond the Pauli limit in high-pressure CeSb₂

Oliver P. Squire,¹ Stephen A. Hodgson,¹ Jiasheng Chen,¹ Vitaly Fedoseev,^{1,*} Christian K. de Podesta,¹ Theodore I. Weinberger,¹ Patricia L. Alireza,¹ and F. Malte Grosche^{1,†}

¹*Cavendish Laboratory, University of Cambridge, Cambridge CB3 0HE, UK*

(Dated: November 3, 2022)

We report the discovery of superconductivity at a pressure-induced magnetic quantum critical point in the Kondo-lattice system CeSb₂, sustained up to magnetic fields that exceed the conventional Pauli limit eight-fold. Like CeRh₂As₂, CeSb₂ is locally non-centrosymmetric around the Ce-site, but the evolution of critical fields and normal state properties as CeSb₂ is tuned through the quantum critical point motivates a fundamentally different explanation for its resilience to applied field.

In an increasing number of materials – notably the new unconventional superconductors CeRh₂As₂ [1] and UTe₂ [2, 3] – superconductivity is surprisingly resilient to magnetic field, and the temperature dependence of the upper critical field shows a rich and unexpected structure. This is important not just for applications in which high magnetic fields are required but also because the field resilience suggests that the superconducting Cooper pairs form triplet states, which may be exploited for quantum computing. In CeRh₂As₂, the postulated high field triplet state has been linked to a structural peculiarity, namely the lack of inversion symmetry around the crucially important Ce atoms, which underpin the electronic structure and the superconducting pairing mechanism.

In the related, clean Kondo lattice material CeSb₂, we here report the discovery of superconductivity over a narrow pressure range that envelops a magnetic quantum critical point (qcp). CeSb₂ displays a complex magnetic phase diagram with at least four magnetic phases and a ferromagnetic ground state [4–8], all of which are initially robust under pressure, but its electronic and magnetic properties change profoundly [9, 10] at the high pressures considered here. Like CeRh₂As₂, high pressure CeSb₂ lacks inversion symmetry around the Ce sites, and its upper critical field is strongly enhanced over expectations from elementary theory. In contrast to CeRh₂As₂, however, signatures of a singlet-triplet transition under applied field are not observed in CeSb₂, suggesting that the critical field is instead boosted by a more general mechanism intrinsic to strong-coupling superconductivity involving ultra-heavy quasiparticles.

Methods. High quality crystals of CeSb₂ with residual resistivity ratios $RRR = \rho_{300}/\rho_0 \simeq 100$ were grown using standard self-flux techniques [5] and characterised by powder x-ray diffraction, resistivity, magnetisation and heat capacity measurements. Piston-cylinder pressure cell measurements up to about 28 kbar were carried out in a compound BeCu/MP35 cell [12] with the superconducting transition temperature of Sn as the pressure gauge [13], whereas a wider pressure range up to 40 kbar was accessed in moissanite anvil cells using room temperature ruby fluorescence to determine the pressure. Glycerol was used as the pressure medium in both types of pres-

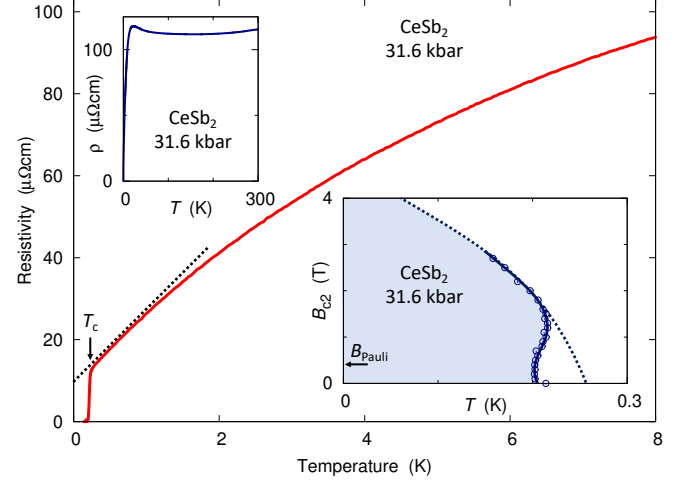


Figure 1. Superconductivity and anomalous normal state in high pressure CeSb₂. The variation of the resistivity ρ with temperature T shows negative curvature all the way down to a sharp transition to $\rho = 0$ at $T_c \simeq 0.22$ K. (left inset) $\rho(T)$ rises sharply to a shoulder at ~ 10 K, reaches a shallow maximum at 22.5 K and then saturates, following a form typical for a Kondo lattice with a low effective bandwidth. (right inset) The resistive upper critical field follows an inverted ‘S’-shape at low fields and at intermediate fields takes on a large negative slope, which would extend to higher T_c (dashed line) without the ‘S’ anomaly. It far exceeds the Pauli paramagnetic limit $B_{\text{Pauli}} \simeq 1.84 \text{ T K}^{-1} T_c(B = 0)$ (horizontal arrow).

sure cell. The crystal orientation reported in magnetic field studies (c -axis vs. in-plane) refers to the low pressure structure. The electrical resistivity was determined using a standard 4-terminal AC technique with a 3 μA current at the lowest temperatures, and the magnetic susceptibility was measured using a mutual inductance technique with a pickup microcoil inside the high pressure sample volume [14]. The heat capacity was obtained from a 3ω temperature modulation technique, oscillating the current in a thick film metal heater and in a Cernox thermometer closely connected to the sample at a frequency ω , and picking up the third harmonic $\omega_3 = 3\omega$ of the resulting thermometer signal [15]. Measurements in a QD PPMS in the range 2 K–300 K were complemented

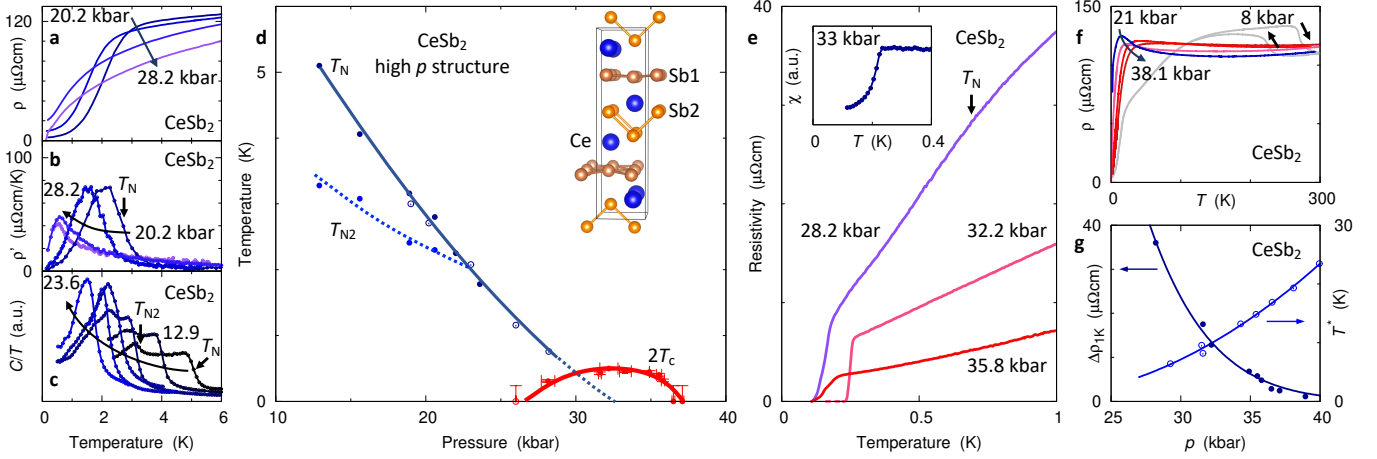


Figure 2. Pressure dependence of magnetic and superconducting states in high pressure CeSb₂. (a-c) Transition anomalies: (a) kink in $\rho(T)$, (b) associated jump in $\rho' = d\rho/dT$, (c) jumps in the heat capacity Sommerfeld ratio C/T . The $\rho(T)$ and $\rho'(T)$ data covers pressures from 20.2 kbar to 28.2 kbar, above which these transition anomalies were no longer resolved. The heat capacity was measured at pressures ranging from 12.9 kbar to 23.6 kbar. It shows a second transition anomaly at a lower temperature T_{N2} , in line with μ SR data [11], which indicates that the low- T state is magnetically ordered. (d) High pressure phase diagram of CeSb₂, showing the gradual suppression of the two magnetic transitions (full circles: from $C(T)$, empty circles: from $\rho(T)$) and a superconducting dome (full/empty symbols from $\rho(T)$ in two different samples, square: from magnetic susceptibility χ as in the inset to panel e). (inset to d) High pressure structure of CeSb₂. (e) $\rho(T)$ at different pressures straddling the qcp, showing the peak T_c at $p_c \simeq 32$ kbar, where a magnetic transition (arrow in 28.2 kbar data) extrapolates to zero, the quasilinear form of $\rho(T)$ at p_c , and the rapid suppression of $\rho(T)$ at low T with increasing pressure. (inset to e) High- p susceptibility data showing the superconducting transition. (f) Normal state resistivity up to room temperature, showing the hysteretic signature of the high T structural transition at 8 kbar (arrows for cooling/warming data) and the very different form of $\rho(T)$ at higher pressures, typical for a Kondo lattice with a low characteristic temperature T^* . We estimate T^* from the shoulder in $\rho(T)$, at which $\rho(T)$ reaches 80% of $\max(\rho)$. (g) Pressure dependence of T^* and of the resistivity increment $\Delta\rho_{1K} = \rho(1K) - \rho_0$, showing the rapid reduction of the T -dependence of $\rho(T)$ at low T and the concomitant increase of T^* with p .

by low temperature studies in a cryogen-free ADR system (Dryogenic Measurement System, DMS) to < 0.1 K and in fields of up to 6 T.

Superconductivity and anomalous normal state.

The normal state in-plane resistivity in CeSb₂ at an applied pressure $p \simeq 31.6$ kbar displays a distinctly non-Fermi liquid, sub-linear temperature dependence $\rho(T)$ (Fig. 1). The resistivity rises steeply at low T and reaches a shallow maximum at 22.5 K, above which it stays roughly constant up to room temperature (left inset in Fig. 1), following a form familiar from other Ce or Yb-based Kondo lattice materials such as CeCu₂Si₂, CeCoIn₅, and YbRh₂Si₂ [16–19]. It approaches saturation well below 10 K, reaching 80% of the maximum resistivity at $T^* \simeq 8.2$ K. These temperatures are similar to those recorded in CeCu₂Si₂, CeCoIn₅ and YbRh₂Si₂, suggesting extremely strong electronic correlations, narrow renormalised bands and high quasiparticle masses in high-pressure CeSb₂.

A sharp resistive transition with mid-point $T_c \simeq 0.22$ K (main plot in Fig. 1) indicates superconductivity at very low temperatures, in line with the low electronic energy scales suggested by the normal state $\rho(T)$. Superconductivity proves surprisingly robust to applied magnetic fields along the crystallographic c direction (right inset

in Fig. 1). It persists to > 3 T at low T , exceeding the Pauli paramagnetic limiting field, which is conventionally written as $B_{\text{Pauli}} = 1.84 \text{ T K}^{-1} T_c$ [20, 21], by nearly an order of magnitude. The in-plane upper critical field is similarly enhanced [15].

For small applied fields, T_c is initially reduced, then rises again to a value slightly higher than the zero-field T_c , for $B \simeq 1.5$ T. This produces an unusual, inverted ‘S’-shaped structure in the $B_{c2}(T)$ curve. The inverted ‘S’ structure is observed at several other pressures ≤ 32.2 kbar but vanishes at higher pressures (see below). The sign reversal of dB_{c2}/dT , which is > 0 over an intermediate field range, points towards an underlying, field tuned phase transition within the normal state [15].

Quantum critical point. Distinct transition anomalies are indeed observed at pressures less than $p_c \simeq 32$ kbar (Fig. 2a-c). Electric transport measurements for $p < p_c$ find a kink in $\rho(T)$ at low T , which causes a jump in the T -derivative of the resistivity $\rho'(T)$ (Fig. 2a-b). Heat capacity measurements under pressure likewise display a jump in $C(T)$ (Fig. 2c) at a transition temperature T_N that is consistent with that of the kink in $\rho(T)$. Heat capacity data furthermore show evidence for a weaker, second transition at a lower temperature T_{N2} , which

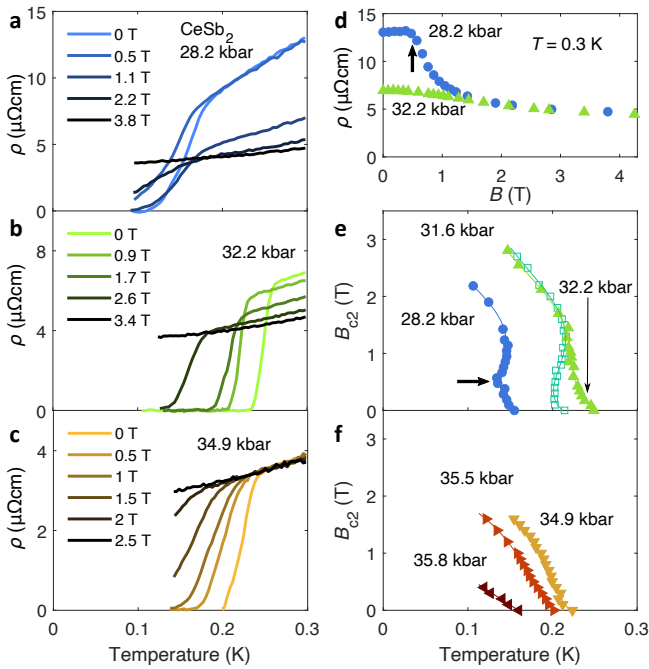


Figure 3. (a-c) Response of the superconducting transition in CeSb₂ to magnetic field applied along the c -axis, for $p < p_c$ (a), for $p \simeq p_c$ (b) and for $p > p_c$ (c). (d) The magnetoresistance at $T > T_c$ displays a distinct kink at $\simeq 0.5$ T (vertical arrow) for $p < p_c$, indicating a field-induced transition out of the magnetically ordered state. (e) $B_{c2}(T)$ curves extracted from the mid-point of the resistive transition display a pronounced inverted ‘S’-shape with a local minimum of T_c at $\simeq 0.5$ T for $p = 28.2$ kbar (horizontal arrow), which corresponds to the kink field in panel (d). (f) At $p > p_c$ the $B_{c2}(T)$ curves revert to a more conventional form.

merges with T_N as pressure is increased. Both step-like heat capacity signatures suggest second-order transitions. High pressure muon spin rotation studies indicate two distinct magnetically ordered states associated with T_N and T_{N2} [11]. The detection of two magnetic transitions is reminiscent of the CeCu₂(Si/Ge)₂ system [22] and of YbRh₂Si₂ under pressure [19]. The magnetic transition signatures extrapolate to zero temperature at a magnetic quantum critical point near 32 kbar. The superconducting transition has likewise been tracked in high pressure transport measurements using two anvil cells and a susceptibility measurement in a third anvil cell (inset of Fig. 2e). Following the magnetic and superconducting transition signatures as functions of pressure results in the phase diagram (Fig. 2d), which shows a superconducting dome tightly confined to the immediate vicinity of a magnetic quantum critical point, indicating a prominent role for magnetic fluctuations in the superconducting pairing mechanism.

Normal and superconducting properties of CeSb₂ evolve rapidly with pressure (Fig. 2e-g). The low T resistivity takes a quasi-linear T dependence near p_c

(Fig. 2e), which saturates to a nearly constant resistivity (Fig. 2f) above a low $T^* \sim 10$ K. The low T slope of $\rho(T)$, measured by the resistivity increment $\Delta\rho_{1K} = \rho(1\text{ K}) - \rho_0$ over the extrapolated residual resistivity ρ_0 diminishes rapidly with increasing pressure. This is accompanied by a steep increase in T^* , demonstrating that compression under applied pressure strongly increases the effective electronic bandwidth in CeSb₂ (Fig. 2g).

High pressure structure. CeSb₂ forms in the orthorhombic SmSb₂ structure (space group 64), which lacks inversion symmetry around the Ce site but is centrosymmetric around the center of the unit cell. Transport measurements at intermediate pressures $6\text{ kbar} < p < 17\text{ kbar}$ show a highly hysteretic resistivity anomaly (e.g. 8 kbar data in Fig. 2f), which shifts to lower temperature with increasing pressure [9] and disappears beyond 17 kbar, where the low- T state differs profoundly from the low- T state at ambient pressure [10]. High pressure X-ray diffraction [11] has established that this anomaly signals a first-order structural phase transition, which at low T is complete by about 17 kbar. The superconducting and magnetic states discussed above are therefore all associated with the high pressure structure of CeSb₂. The rare earth (R) diantimonides RSb₂ adopt a variety of structure types, all of which lack inversion symmetry around the rare earth site: SmSb₂ (like CeSb₂ at $p = 0$), HoSb₂ (orthorhombic, space-group 21), EuSb₂ (monoclinic, space-group 11) and YbSb₂ (orthorhombic, space-group 63). The X-ray data and *ab initio* DFT calculations in [11] unambiguously rule out the SmSb₂ and HoSb₂ structures for high pressure CeSb₂ and favour the YbSb₂ structure (inset in Fig. 2d).

Critical fields. The locally non-centrosymmetric structure of high pressure CeSb₂ invites comparison to CeRh₂As₂ [1, 23–27] and other unconventional superconductors such as UTe₂, UGe₂ and UPT₃ (e.g. [28]) when considering the response to applied magnetic field. Both the form of the critical field curve $B_{c2}(T)$ in CeSb₂ and the magnitude of the upper critical field are unusual. We consider first the inverted ‘S’-shaped form for $B_{c2}(T)$ displayed in the inset of Fig. 1. The initial reduction, then increase of T_c with field is most pronounced at the lowest pressure at which full resistive transitions could be observed (28.2 kbar, Fig. 3a). It is already weaker at 31.6 kbar (Fig. 1) and weaker still close to the qcp, at 32.2 kbar (Fig. 3b, e). Comparing $B_{c2}(T)$ at these last two pressures (Fig. 3e) shows that near the qcp, the critical field curves converge on a single line at high fields but differ at low fields. At pressures above p_c , the critical field curves gradually change into the conventional form (Fig. 3f). The relative reduction of T_c at low fields < 0.5 T for $p < p_c$ could be seen as a signature of a field-induced transition between two distinct superconducting states, as in CeRh₂As₂ [1], or it might result from a field-induced magnetic transition. The step-like

Table I. Critical field data for selected heavy fermion superconductors. T_c , initial slope of the upper critical field B'_{c2} , experimental B_{c2} in the low- T limit and C/T at T_c have been extracted from the literature. The Pauli limit B_{Pauli} is calculated as $1.84 \text{ T K}^{-1} T_c$. Elementary theory predicts that $\sqrt{B'_{c2}/T_c} \propto C/T$ [15], as is indeed roughly confirmed by the tabulated data. Applying this analysis to CeSb₂ near p_c , at 34.9 kbar, produces an estimate for C/T of $\sim 1.2 \text{ J/molK}^2$.

	T_c K	B'_{c2} T/K	B_{Pauli} T	$B_{c2}(0)$ T	$\sqrt{B'_{c2}/T_c}$ $\text{T}^{1/2}/\text{K}$	C/T J/molK^2
CeCoIn ₅ [30]	2.2	30.5	4.05	11.5	3.7	0.3
CeCu ₂ Si ₂ [31]	0.6	35	1.10	1.9	7.6	0.7
CeRh ₂ As ₂ [1]	0.26	97	0.48	14	19.3	2
CeSb ₂ ($\simeq p_c$)	0.22	30	0.40	> 3	11.8	1.2 (est.)
UPt ₃ [32]	0.52	6.3	0.96	1.8	3.5	0.4
UBe ₁₃ [33]	0.95	45	1.75	14	6.9	1

magnetoresistance anomaly at 28.2 kbar shown in Fig. 3d points towards the second scenario. The transition field of $\simeq 0.5 \text{ T}$ (vertical arrow) corresponds to the minimum T_c in the 28.2 kbar critical field curve in Fig. 3e (horizontal arrow). These findings suggest that the inverted ‘S’ shape of $B_{c2}(T)$ on the ordered side of the qcp results from the interplay between applied field and the magnetic spin fluctuation spectrum: tuning the system out of the magnetically ordered state with increasing field enhances order parameter fluctuations and the associated pairing interaction, thereby strengthening superconductivity. A similar explanation has been advanced in pressurised UGe₂ [29].

Considering next the eight-fold enhancement of B_{c2} over the conventional Pauli limit $B_{\text{Pauli}} = 1.84 \text{ T K}^{-1} T_c$ [21, 34] in CeSb₂, we note that moderate violations of the Pauli limit are common in Ce-based heavy fermion materials such as CeCoIn₅ and CeCu₂Si₂ (Table I) without necessarily being taken as evidence for triplet pairing. The ratio of the high initial slope B'_{c2} over T_c in compressed CeSb₂ indicates a very high Sommerfeld ratio $C/T \sim 1.2 \text{ J/molK}^2$ (Table I) [15]. It is larger than the corresponding ratios in UPt₃, CeCoIn₅, CeCu₂Si₂, and UBe₁₃, suggesting that the quasiparticles underlying superconductivity in high pressure CeSb₂ are among the heaviest ever recorded in a superconducting heavy fermion material. This is significant, because theoretical studies [35, 36] indicate that violations of Pauli limiting may generally be expected in superconductors with large mass renormalisation, irrespective of whether the pairing is mediated by phonons or spin-fluctuations and whether the pairing state has *s*-wave or *d*-wave symmetry [37]. The original calculation of the conventional Pauli limiting field [21, 34] balances the superconducting condensation energy against the magnetic energy involved in changing the spin alignment of the paired electrons in an applied field. The former depends on the energy gap, the latter on the spin susceptibility. Although some uncertainty in the latter arises from imprecise knowledge

of the conduction electron *g*-factor, this would have to be $\ll 1$ to explain substantially enhanced Pauli limiting fields, which is difficult to justify: strong anisotropy of the *g*-factor is ruled out by the large B_{c2} observed for $B \perp c$ [15]. In strong-coupling superconductors the balance between condensation energy and magnetic energy needs to be modified both on the side of the condensation energy, because the energy gap may be far larger than the BCS relation $\Delta = 1.76 k_B T_c$ suggests, and on the side of the magnetic energy, because the spin susceptibility is reduced below the Pauli susceptibility indicated by the quasiparticle density of states by as much as the interaction-induced mass enhancement. In model calculations, this causes the Pauli limit to be boosted to about $1.5 \text{ T K}^{-1} T_c m^*/m_b$, with m^* the renormalised quasiparticle mass and m_b the bare band mass [35]. In UBe₁₃, the eight-fold enhancement of B_{c2} over the conventional Pauli limit (Table I) has been interpreted likewise [33] in terms of a strong-coupling calculation, and a similar boost to the limiting field was found in a calculation for spin-fluctuation induced *d*-wave pairing [37]. In this approach, resilience to high fields is achieved by gradually admixing a frequency-odd triplet pairing state into the underlying frequency-even singlet pairing state [38, 39] (see also [40, 41] for material-specific calculations). This general route contrasts starkly with the scenario advanced for CeRh₂As₂ (e.g. [1]), which is predicated on its locally non-centrosymmetric structure. In heavy fermion materials such as CeSb₂, a quantitative calculation is hindered by the similar magnitudes of the Zeeman energy at B_{c2} and electronic as well as bosonic energy scales, by the effect of the applied field on the pairing interaction, by the highly anomalous normal state, which deviates profoundly from expectations of Fermi liquid theory, and by our incomplete understanding of the origins of mass renormalization and pairing interaction, which do not align completely. The intriguing suggestion that increasing admixture of odd-frequency, triplet superconductivity can boost the critical field in strongly correlated materials should be tested in more detailed theoretical and computational investigations.

High-pressure CeSb₂ emerges as a clean, ultra-heavy fermion system with superconductivity forming out of a pronounced non-Fermi liquid state and an upper critical field far beyond the Pauli limit. Because the qcp underlying the superconducting dome can in CeSb₂ be crossed under pressure, this material supplies an excellent test case for refining our understanding of unconventional superconductivity. Our findings suggest that strong mass renormalization boosts the magnitude of B_{c2} without the need for a singlet-triplet phase transition as reported in CeRh₂As₂, and that the interplay between applied field, magnetic order and the associated magnetic fluctuations can explain the evolution of $B_{c2}(T)$ across the qcp.

We thank, in particular, A. Chubukov and G. Lonzarich for helpful discussions and Z. Feng and Y. Zou for

early work on the structural and magnetic transitions in CeSb₂. The project was supported by the EPSRC of the UK (grants no. EP/K012894 and EP/P023290/1) and by Trinity College.

* Now at Dept. of Physics, Massachusetts Institute of Technology, Cambridge, MA 02139, USA

† fmg12@cam.ac.uk

- [1] S. Khim, J. Landaeta, J. Banda, N. Bannor, M. Brando, P. Brydon, D. Hafner, R. K  chler, R. Cardoso-Gil, U. Stockert, A. P. Mackenzie, D. F. Agterberg, C. Geibel, and E. Hassinger, *Science* **373**, 1012 (2021).
- [2] S. Ran, C. Eckberg, Q.-P. Ding, Y. Furukawa, T. Metz, S. R. Saha, I.-L. Liu, M. Zic, H. Kim, J. Paglione, and N. P. Butch, *Science* **365**, 684 (2019).
- [3] D. Aoki, A. Nakamura, F. Honda, D. Li, Y. Homma, Y. Shimizu, Y. J. Sato, G. Knebel, J.-P. Brison, A. Pourret, D. Braithwaite, G. Lapertot, Q. Niu, M. Valiska, H. Harima, and J. Flouquet, *J. Phys. Soc. Jpn.* **88**, 043702 (2019).
- [4] P. C. Canfield, J. D. Thompson, and Z. Fisk, *Journal of Applied Physics* **70**, 5992 (1991).
- [5] S. L. Bud'ko, P. C. Canfield, C. H. Mielke, and A. H. Lacerda, *Phys. Rev. B* **57**, 13624 (1998).
- [6] Y. Zhang, X. Zhu, B. Hu, S. Tan, D. Xie, W. Feng, L. Qin, W. Zhang, Y. Liu, H. Song, L. Luo, Z. Zhang, and X. Lai, *Chinese Phys. B* **26**, 067102 (2017).
- [7] B. Liu, L. Wang, I. Radelytskyi, Y. Zhang, M. Meven, H. Deng, F. Zhu, Y. Su, X. Zhu, S. Tan, and A. Schneidewind, *J. Phys.: Condens. Matter* **32**, 405605 (2020).
- [8] C. Trainer, C. Abel, S. L. Bud'ko, P. C. Canfield, and P. Wahl, *Phys. Rev. B* **104**, 205134 (2021).
- [9] T. Kagayama, G. Oomi, S. Bud'ko, and P. Canfield, *Physica B: Condensed Matter* **281**, 90 (2000).
- [10] T. Kagayama, Y. Uwatoko, S. Bud'ko, and P. Canfield, *Physica B: Condensed Matter* **359–361**, 320 (2005).
- [11] C. de Podesta, T. Weinberger, O. Squire, Z. Feng, J. Chen, G. I. Lampronti, R. Khasanov, and F. M. Grosche, to be publ. (2022).
- [12] I. R. Walker, *Rev. Sci. Instrum.* **70**, 3402 (1999).
- [13] T. Smith, C. Chu, and M. Maple, *Cryogenics* **9**, 53 (1969).
- [14] P. L. Alireza and S. R. Julian, *Rev. Sci. Instr.* **74**, 4728 (2003).
- [15] See Supplementary Material at [URL], which includes Refs. [42–46] for further details of the in-plane critical field, estimates based on the critical field data, implications of the sign-reversal of $B'_{c2}(T)$, and the temperature modulation heat capacity method (2022).
- [16] B. Bellarbi, A. Benoit, D. Jaccard, J. M. Mignot, and H. F. Braun, *Phys. Rev. B* **30**, 1182 (1984).
- [17] C. Petrovic, P. G. Pagliuso, M. F. Hundley, R. Movshovich, J. L. Sarrao, J. D. Thompson, Z. Fisk, and P. Monthoux, *J. Phys.: Condens. Matter* **13**, L337 (2001).
- [18] A. Malinowski, M. F. Hundley, C. Capan, F. Ronning, R. Movshovich, N. O. Moreno, J. L. Sarrao, and J. D. Thompson, *Phys. Rev. B* **72**, 184506 (2005).
- [19] O. Trovarelli, C. Geibel, S. Mederle, C. Langhammer, F. M. Grosche, P. Gegenwart, M. Lang, G. Sparn, and F. Steglich, *Phys. Rev. Lett.* **85**, 626 (2000).
- [20] A. M. Clogston, *Phys. Rev. Lett.* **9**, 266 (1962).
- [21] B. S. Chandrasekhar, *Appl. Phys. Lett.* **1**, 7 (1962).
- [22] H. Yuan, F. Grosche, M. Deppe, C. Geibel, G. Sparn, and F. Steglich, *Science* **302**, 2104 (2003).
- [23] D. M  ckli and A. Ramires, *Physical Review B* **104**, 134517 (2021).
- [24] J. F. Landaeta, P. Khanenko, D. C. Cavanagh, C. Geibel, S. Khim, S. Mishra, I. Sheikin, P. M. R. Brydon, D. F. Agterberg, M. Brando, and E. Hassinger, *ArXiv220407975 Cond-Mat* (2022).
- [25] D. C. Cavanagh, T. Shishidou, M. Weinert, P. M. R. Brydon, and D. F. Agterberg, *Phys. Rev. B* **105**, L020505 (2022).
- [26] D. Hafner, P. Khanenko, E.-O. Eljaouhari, R. K  chler, J. Banda, N. Bannor, T. L  hmann, J. Landaeta, S. Mishra, I. Sheikin, E. Hassinger, S. Khim, C. Geibel, G. Zwicknagl, and M. Brando, *Physical Review X* **12**, 011023 (2022).
- [27] M. Kibune, S. Kitagawa, K. Kinjo, S. Ogata, M. Manago, T. Taniguchi, K. Ishida, M. Brando, E. Hassinger, H. Rosner, C. Geibel, and S. Khim, *Physical Review Letters* **128**, 057002 (2022).
- [28] T. Hazra and P. Coleman, *arXiv:2205.13529* (2022).
- [29] I. Sheikin, A. Huxley, D. Braithwaite, J. Brison, S. Watanabe, K. Miyake, and J. Flouquet, *Phys. Rev. B* **64**, 220503R (2001).
- [30] C. F. Miclea, M. Nicklas, D. Parker, K. Maki, J. L. Sarrao, J. D. Thompson, G. Sparn, and F. Steglich, *Phys. Rev. Lett.* **96**, 117001 (2006).
- [31] S. Kittaka, Y. Aoki, Y. Shimura, T. Sakakibara, S. Seiro, C. Geibel, F. Steglich, Y. Tsutsumi, H. Ikeda, and K. Machida, *Phys. Rev. B* **94**, 054514 (2016).
- [32] J. W. Chen, S. E. Lambert, M. B. Maple, Z. Fisk, J. L. Smith, G. R. Stewart, and J. O. Willis, *Phys. Rev. B* **30**, 1583 (1984).
- [33] F. Thomas, B. Wand, T. L  hmann, P. Gegenwart, G. R. Stewart, F. Steglich, J. P. Brison, A. Buzdin, L. Gl  mot, and J. Flouquet, *J. Low Temp. Phys.* **102**, 117 (1996).
- [34] A. M. Clogston, A. C. Gossard, V. Jaccarino, and Y. Yafet, *Phys. Rev. Lett.* **9**, 262 (1962).
- [35] M. Schossmann and J. P. Carbotte, *Phys. Rev. B* **39**, 4210 (1989).
- [36] J. P. Carbotte, *Rev. Mod. Phys.* **62**, 1027 (1990).
- [37] A. P  rez-Gonz  lez, *Physical Review B* **54**, 16053 (1996).
- [38] M. Schossmann and E. Schachinger, *Phys. Rev. B* **33**, 6123 (1986).
- [39] M. Matsumoto, M. Koga, and H. Kusunose, *J. Phys. Soc. Jpn.* **81**, 033702 (2012).
- [40] A. Aperis, P. Maldonado, and P. M. Oppeneer, *Phys. Rev. B* **92**, 054516 (2015).
- [41] A. Aperis, E. V. Morooka, and P. M. Oppeneer, *Annals of Physics* **417**, 168095 (2020).
- [42] E. Helfand and N. R. Werthamer, *Phys. Rev.* **147**, 288 (1966).
- [43] M. Tinkham, *Introduction to Superconductivity* (Dover Publications, 2004).
- [44] T. P. Orlando, E. J. McNiff, S. Foner, and M. R. Beasley, *Phys. Rev. B* **19**, 4545 (1979).
- [45] P. F. Sullivan and G. Seidel, *Physical Review* **173**, 679 (1968).
- [46] E. Gati, G. Drachuck, L. Xiang, L.-L. Wang, S. L. Bud'ko, and P. C. Canfield, *Review of Scientific Instruments* **90**, 023911 (2019).